JOURNAL OF RAMAN SPECTROSCOPY, VOL. 25, 13–23 (1994)

REVIEW

Applications of Raman and Surface-Enhanced Raman Scattering Spectroscopy in Medicine

Igor Nabiev,* Igor Chourpa and Michel Manfait†
Laboratoire de Spectroscopie Biomoléculaire, UFR de Pharmacie, Université de Reims, 51 rue Cognacq-Jay, F-51096 Reims Cedex, France

The first part of this review is devoted to medical applications of Raman spectroscopy as a diagnostic or analytical tool. Studies of human arteries, ocular lenses, living cells and chromosomes are reviewed, in addition to recent advantages in cancer diagnostics using Raman spectroscopy. The second and major part is devoted to a relatively new field, surface-enhanced Raman scattering (SERS) spectroscopy of biomedical species. The SERS effect is accompanied by strong quenching of fluorescence and so enabes the range of species that can be investigated by Raman technique to be extended. The ultra-high sensitivity of SERS enables spectra to be obtained at concentrations down to 10^{-10} M. A wide range of experiments designed to probe the structure, topology and composition of biomedical species using SERS spectroscopy can be envisioned. Some of these currently being studied are: the determination of the distribution of drugs within a living cell and on the cellular membrane, the selective study of cell membrane components, the analysis of crude biomedical mixtures and extracts and new techniques, based on SERS spectroscopy, Fourier transform SERS spectroscopy and the SERS microprobe method.

INTRODUCTION

Optical spectroscopy provides new ways to study physical and chemical changes occurring in tissues, cells and chromosomes, and thereby offers exciting possibilities in diagnostics and therapeutics. There are several optical techniques available, such as spectrofluorimetry, infrared spectroscopy, circular dichroism and Raman spectrocopy, that are sensitive to the chemical composition and structure of biomedical species. Compared with the other optical techniques, Raman spectroscopy has excellent fingerprinting capabilities. It can be utilized *in situ* under physiological experimental conditions and when resonance Raman scattering can be used it is extremely selective. By coupling a confocal optical microscope to a conventional Raman spectrometer, Raman spectroscopy becomes a microprobe with a spatial resolution of less than 1 μm.

Medical applications of Raman spectroscopy as a diagnostic or analytical tool began to appear in the mid-1970s. The pioneering work of Yu *et al.*[1] showed that Raman spectra could be obtained from eye lenses. Hartman *et al.*[2] published the first Raman spectra from intact viruses. The laser Raman microprobe has been used for histological examination of various pathologies.[3]

There are, however, some problems in the applications of Raman spectroscopy in biomedicine. These include the small Raman scattering cross-section, which results in low signal levels, the possibility of sample damage and the strong fluorescence background from crude biomedical extracts and mixtures, tissues and cells. The problem of sample damage can be addressed by optimization of the experimental conditions, spinning solid samples or flowing liquid samples, cooling (for thermal damage problems) and placing samples in a vacuum or in an inert environment such as nitrogen (for photo-oxidation problems). The problem of fluorescence background can be circumvented by recognizing that most materials, including tissue, exhibit virtually no fluorescence emission with near-infrared (NIR) irradiation. This has led several groups to examine the prospects of extracting histochemical information from human tissue using NIR–Raman and NIR–Fourier transform (FT) Raman spectroscopy.[4–6] The problem of the low sensitivity of Raman spectroscopy can be solved in two ways. One is to improve the sensitivity of the instrumentation. This has been achieved in Greve's laboratory[7–12] by the construction of a very sensitive confocal Raman microspectrometer[7–9] enabling excellent Raman spectra to be recorded from single cells and chromosomes,[9–11] and the detection of the intracellular location of carotenoids,[12] etc.

The other method is to enhance the Raman signal. To study nucleic acids and proteins within the biomedical species, that means using UV excitation.[13,14] With recently developed UV Raman spectrometers it has been shown that single-cell resonance Raman spectra could be obtained in this way.[15] However, the increased risk of UV radiation-induced damage has to be kept in mind and the fluorescence background strongly interferes with the Raman spectra. Another approach is based on the utilization of surface-enhanced Raman scattering (SERS). The efforts of Koglin and Sequaris,[16] Cotton *et al.*[17–19] and Nabiev and coworkers[20–23] have led to the development of a new spectroscopic technique for biomedical studies, enabling the effective Raman cross-section to be increased by a

* Permanent address: Optical Spectroscopy Division, Shemyakin Institute of Bioorganic Chemistry, Russian Academy of Sciences, ul.Miklukho-Maklaya 16/10, 117871 Moscow, Russia.
† Author to whom correspondence should be addressed.

0377-0486/94/010013-11 $10.50

Received 15 July 1993
Accepted 1 October 1993

factor of 10^8 and background fluorescence to be quenched.

The review is divided into two major parts. First, an overview of applications of conventional, resonance and micro-Raman spectroscopy in biomedical studies of the human eye, breast and aorta tissues, cells and chromosomes is given. Biomedical applications of SERS, micro-SERS and FT-SERS spectroscopy, with emphasis on applications related to cancer research, are summarized in the second part. Because a number of comprehensive reviews have described physical and theoretical aspects of SERS,[24–26] the most common SERS-active substrates[23,25–27] and their applications to isolated and purified biological molecules,[16–23] no attempt will be made to discuss work in this field. The major focus will be given to the newest medical applications of Raman and SERS spectroscopy. The general objective is to show that various Raman techniques have great potential for medical diagnostic and analytical applications.

RAMAN AND MICRO-RAMAN SPECTROSCOPY IN MEDICINE

The major limitation in the use of Raman spectroscopy as a medical tool has been the interference of the intrinsic fluorescence present in most tissues, cells, lenses, etc., which obscures the Raman signal. That is why only a few attempts at medical applications were reported up to the end of the 1980s.[28,29] NIT–FT-Raman spectroscopy, which has been developed recently, enables this problem of conventional Raman spectroscopy to be circumvented.

Cancer diagnostics

Currently, there are no methods available for the early detection and rapid histoligical diagnosis of cancer. The early detection of gynecologic cancers is a medical priority because their incidence represents about 15% of all cancers.[30] Recently, Liu *et al.*[31] used FT-Raman spectroscopy as a diagnostic tool for cancer detection in gynecological tracts.

Liu *et al.*[31] recorded excellent NIR–FT-Raman spectra from malignant and non-malignant (normal and benign) samples from patients with neoplasms during diagnostic or therapeutic procedures. They screened tissues from the cervix, uterus, endometrium, ovary and breast. Pronounced differences were observed between the cancer, benign and normal tissue spectra. For example, FT-Raman spectra from cancerous tissue with fat around it, normal breast tissue and cancerous endometrium are presented in Fig. 1. Normal tissue shows a Raman band at *ca.* 1445 cm^{-1}. In the breast and endometrial cancer, this line is stronger compared with normal tissues and shifted to 1437 and 1435 cm^{-1}, respectively. Comparison of spectra from tissues and from model compounds shows that the line at *ca.* 1437 cm^{-1} from the fat around the cancerous breast tissues (Fig. 1) may be from cholesterol.

On the basis of FT-Raman data from tissues of patients at different stages of gynecological cancer and the results of biodiagnostics, Liu *et al.*[31] concluded that

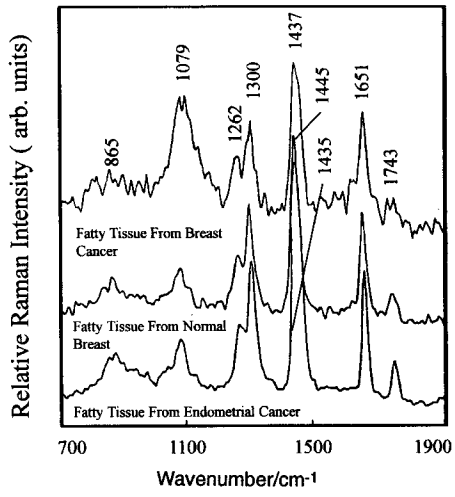

Figure 1. IR-FT Raman spectra from fatty tissues of cancer and normal breast and endometrial cancer. The upper spectrum is from the fatty tissue of breast cancer, the middle spectrum is from the fatty tissue of normal breast and the lower spectrum is from the fatty tissue of endometrial cancer. Six identical Raman peaks at 1743, 1651, 1300, 1262, 1079, and 865 cm^{-1} are observed for the three fatty tissues. Only one characteristic Raman line is different for normal and cancer tissues. For the normal tissue the band is at 1445 cm^{-1} and for the cancerous tissues of either breast or endometrium the band shifts to 1437 and 1435 cm^{-1}. A Bomem DA 3.16 FT-Raman spectrometer was used. A 1064 nm CW Nd:YAG laser (1 W) was used for exciting samples. Spectra are the sum of 800 scans. The samples were irregular slices of tissue with dimensions 10 × (6–10) × (3–8) mm^3. An area of 6 × 6 mm^2 was scanned for each measurement. Reproduced with permission from Liu *et al.*[31] Copyright (1992) Elsevier Sequoia.

NIR–FT-Raman spectroscopy can (a) locate the tumour with an accuracy of less than a few hundred micrometres (b) detect gynecological tract cancer at an early stage and (c) probe a gynecological tract directly using an endoscope. Moreover, endoscopes with a needle can be used to investigate the state of internal organs, such as the ovaries.[31]

Human arteries

Detailed information on atherosclerotic tissue can be obtained by Raman spectroscopy without sample preparation, specimen degradation or fluorescence interference when NIR excitation wavelengths are employed.[32,33] Utilizing a spectrograph–CCD system, Baraga *et al.*[34] have demonstrated that NIR Raman spectra can be collected rapidly from a human artery and this allows data to be collected *in vivo*. The same group demonstrated that Raman spectroscopy can be employed to determine collagen, elastin, cholesterol, cholesterol esters, triglycerides, calcium hydroxyapatite, carbonated apatites and carotenoids in normal and atherosclerotic arteries.[32–34]

NIR–Raman spectra obtained from typical specimens of normal, atheromatous and calcified human aorta are shown in Fig. 2. Manoharan *et al.*[35] demonstrated that the Raman spectrum of normal aorta is dominated by bands due to proteins whereas the bands due to proteoglycans, which are known to make up the group substance in an artery wall, do not contribute to the spectra. The spectrum of the atheromatous plaque is distinctly different from that of normal aorta [Fig. 2(b)]

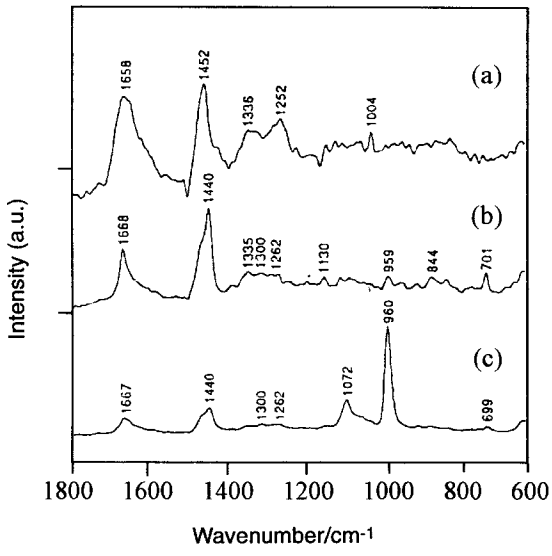

Figure 2. NIR–Raman spectra of (a) normal aorta (×8), (b) atheromatous plaque (×4) and (c) calcified plaque. A Perkin-Elmer FT-IR spectrometer with a Raman accessory was utilized. A 1064 nm CW Nd:YAG laser (400 mW in a 1 mm diameter spot on the sample) was used for exciting samples. Spectra are the sum of 512 scans (35 min collection time). Reproduced with permission from Manoharan *et al.*[35] Copyright (1992) Elsevier Sequoia.

and shows many of the bands assignable to cholesterol and its esters. It is also possible to distinguish between triglyceride contributions in the NIR Raman spectra of atheromatous plaques. Finally, the NIR–Raman spectrum of calcified plaques [Fig. 2(c)] shows a significant contribution from calcium hydroxyapatite (960 cm^{-1}) and carbonate apatites (1070 cm^{-1}).[34]

Manoharan *et al.*[35] have developed a method for the quantitative analysis of the histochemical composition of human artery. They evaluated the Raman scattering cross-sections of different bands from proteins, collagen and elastin, cholesterol lipids and calcium hydroxyapatite. These compounds were found to be the main contributors to bands observed in the Raman spectra of normal and atherosclerotic aorta. Using these data, quantitative information regarding the relative concentration of biological constituents in different types of atherosclerotic aorta has been extracted.

Ocular lenses

The ocular lens is a good object to investigate non-destructively by mean of laser Raman spectroscopy.[28] The lens is a highly organized transparent organ which consists of the tissues from the embryonal stage in the nucleus centre to a newly differentiated stage in the equatorial region. The lens itself shows ageing with very old tissues in the centre to very young tissues in the equator. Since lens proteins are highly packed, especially in the nucleus centre, a good Raman spectrum can be obtained from the lens proteins in the lens *in situ*. It has been stated that a useful Raman spectrum can be recorded from a volume of 10^{-3} μl,[36] with only 1 mW of laser power and with a data integration time of *ca.* 700–950 s. Therefore this seems to be a useful method for investigating macromolecular alterations in opaque cataractous spots. It is also considered to be a promising clinical diagnostic tool for senile cataract.[37]

Raman spectra of intact human lenses have been recorded by several investigators.[28,29,38,39] They were confronted with the problems of excessive fluorescence in human lenses above the age of 20 yr. In order to erase the excessive fluorescence, a clear region in the intact lens was irradiated with laser light for many hours before recording a spectrum. Difficulties regarding the precise focusing on opaque and translucent regions were overcome by Yu *et al.*[40] by developing a fluorescence–Raman imaging system which scans the surface of the lens and is therefore not affected by opaque regions in the body of the lens, a great advantage for cataract research.

To improve the accuracy in the location of the spot measured by Raman spectroscopy and to avoid the problem of Raman signals being overwhelmed by fluorescence for human lenses over the age of 20–30 yr, lens slices have been used.[39] Lens slices even of very old human lenses give reliable Raman spectra, provided that they are pre-irradiated with laser light for several hours. The Raman spectra thus obtained were qualitatively fully comparable to those obtained from young non-fluorescent human lenses. A main factor involved in the lower fluorescence of slices is that in a slice less fluorescent material is excited and that consequently the backscattering of fluorescent light from positions outside the measured volume into the objective will be less. In addition, the absorption of Raman and laser light above the focused spot has been found to be less in a slice.

Cells and chromosomes

A method for improving the sensitivity of Raman instrumentation has been achieved in Greve's laboratory by the construction of a very sensitive confocal Raman microspectrometer enabling Raman spectra to be recorded from single cells and chromosomes.[7–9] The main features of the instrument are as follows: (a) high signal throughput from the microscope objective to the detector (40%); (b) sensitive, essentially photon noise-limited signal detection by means of a liquid nitrogen-cooled CCD camera (quantum efficiency 40% at 700 nm, 10 electrons of read-out noise per channel and negligible dark current); (c) confocal signal detection, leading to effective suppression of background Raman signals from substrates or buffer (spatial resolution *ca.* 0.45 × 0.45 × 1.3 μm); and (d) laser radiation of 660 nm was used to prevent radiation damage of the samples.

Puppels *et al.*[10] narrowed the range of potential mechanisms of damage of biological samples and optimized the experimental conditions for studies of single living cells, chromosomes, granulocytes, etc. They used high numerical aperture objectives which focus the laser light into a spot *ca.* 0.5 μm in diameter. This leads to a high irradiance of 0.25–10 MW cm^{-2} for 0.5–20 mW of laser power. The degradation of cells and chromosomes under the influence of 514.5 nm laser radiation was accompanied by a gradual decrease in the intensity of the Raman signal and was observed at all laser powers tested. It is interesting that for model solutions of isolated DNA and histone protein irradiated for 3 h with a

laser power of 25 mW (12.5 MW cm^{-2}) at 514.5 nm, no signs of sample degradation were found. No bleaching effects for cells and chromosomes were observed using laser radiation at 632.8 or 660 nm. It is clear that laser radiations at 632.8 and 660 nm is much less harmful than that at 514.5 nm.

The contribution to sample degradation of processes of multiphoton absorption and sample and substrate heating has been carefully analysed and excluded.[10] It was found that the amount of damage depends only on the total laser radiation dose and not on the intensity of the laser radiation. One-photon laser radiation absorption by the chromosomes and cells remains the only possible process involved in sample degradation. The fact that CT-DNA and histone, two of the main chromosome constituents, in their purified form are not susceptible to radiation damage (even at 514.5 nm) has shown that other compounds acting as photosentitizers must be present in chromosomes and cells. Such sentitizers (e.g. flavins in the cell enzymes) do not absorb light in the red region, because excitation of the spectra with laser radiation of 660 nm does not induce sample degradation. Green laser excitation brings the sentitizer via the singlet state for a long-lived triplet state. It can then react with an oxygen molecule to form singlet oxygen or a superoxide ion. The reactive oxygen species could cause the observed radiation damage, through oxidation of the DNA bases or amino acids, leading to lesions in these molecules.

Thus, to preserve a biomedical sample from degradation, the use of red excitation for conventional Raman microprobe spectroscopy or depositing the samples in an inert medium if shorter wavelength excitations is necessary is strongly recommended.

Puppels *et al.*[10] described a Raman microspectroscopic investigation of human granulocytes, the cells with the dense granulation of the cytoplasm. The Raman spectrum of the nucleus consisted of lines that can be assigned to DNA and protein vibrations and strongly resembles reported spectra of isolated chromatin and a single metaphase chromosome. The cytoplasm spectra differed substantially from that of the nucleus. The amount of DNA present in the measured volume during the recording of a spectrum from chromosomes was estimated to be *ca* 50 fg, corresponding to 50×10^6 base pairs.

Puppels *et al.*[9] also recorded an excellent Raman spectrum of metaphase chromosomes which they used to obtain a better understanding of the origins of the band patterns that appear after physico-chemical treatment and staining. They measured the differences in the DNA/protein ratio between band, interband and a telomer of a fixed polytene chromosome. They investigated the possibility that these differences are related to local variations in transcriptional activity by also studying unfixed chromosomes. They studied the presence and induction of left-handed (*Z*)-DNA in such chromosomes.

A vast range of applications of the instrument developed by Greve and co-workers in the analysis of small biological structures and possibly for monitoring biological events, such as the cytotoxic process mediated by natural killer cells, can be expected. The use of 660 nm laser radiation permits Raman measurements on cells and chromosomes which have been labelled with fluorescein-conjugated antibodies, thus facilitating the prior localization of specific structures such as sites of transcription or replication by conventional fluorescence microscopy. The combination with immunofluorescence techniques thus further increases the potential of Raman microprobe biomedical applications.

Very recently the presence and subcellular location of carotenoids in human lymphocyte subpopulations and natural killer cells has been studied.[12] The focal point of carotenoid concentration in helper–inducer T-lymphocytes, in cytotoxic–suppressor T-lymphocytes and in natural killer cells was found to be in the Gall body (Fig. 3). Comparison of the intensities of the carotenoid Raman signal obtained from Gall bodies [Fig. 3(B)] and that of a β-carotene solution [Fig. 3(A)] allows the evaluation of the concentration of carot-

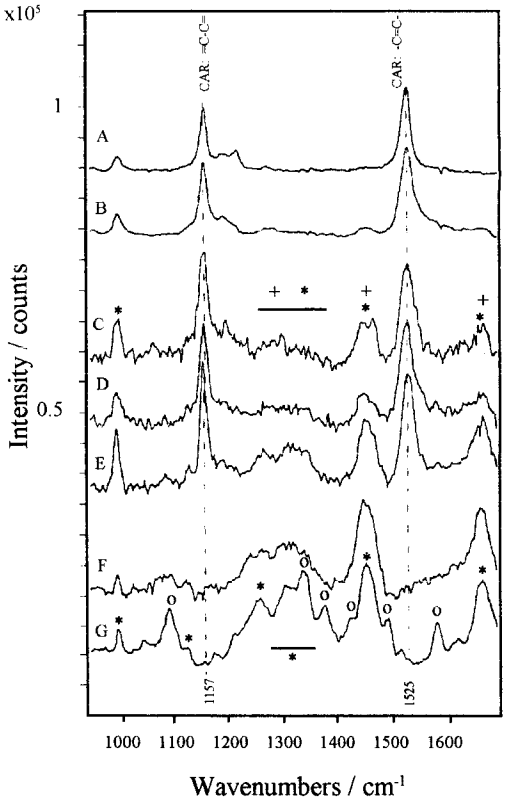

Figure 3. Raman spectra of β-carotene, human T-lymphocytes and natural killer cells. (A) β-Carotene solution in chloroform (0.5 mg ml^{-1}). (B) Helper–inducer T-lymphocyte: spectrum obtained from Gall body. (C) Natural killer cell: spectrum obtained in the cytoplasm, apparently from the Golgi complex. (D) Cytotoxic–suppressor T-lymphocyte: spectrum obtained in the cytoplasm, apparently from the Golgi complex. (E) $T_{\gamma\delta}$-lymphocyte: spectrum obtained in the cytoplasm, apparently from the Golgi complex. (F) B-lymphocyte: characteristic cytoplasmic Raman spectrum (average of nine measurements), containing protein and phospholipid signal contributions,[8–10] but lacking a carotenoid signal. (G) Nuclear Raman spectrum: average of ten measurements in different types of lymphocytes and natural killer cells, containing DNA and protein signal contributions,[8,9,11] but lacking a carotenoid signal. CAR = carotenoid. (*) Protein signal contribution; (+) phospholipid signal contribution; (○) DNA signal contribution. Conditions: laser power 5–6 mW (on sample); signal integration time for each measurement 30 s; cells on poly-L-lysine-coated fused-silica substrates and immersed in Hank's buffered salt solution (HBSS, according to GIBCO 041-04025, phenol red omitted). The intensity scale is for spectra A and B; the multiplication factor for spectra C–G is 8. Reproduced with permission from Puppels *et al.*[12] Copyright (1993) Wiley–Liss, Inc.

enoids within the Gall bodies. This was found to be three orders of magnitude higher than that in blood plasma. On the other hand, in most measurements on B-lymphocytes, no carotenoid signal was found, although they also possess a well developed Golgi complex. The results demonstrated the possibility of investigating the mechanisms behind the suggested protective role of carotenoids against the development of cancers.

SERS AND MICRO-SERS SPECTROSCOPY IN MEDICINE

The instrumentation required for SERS is simple and similar to that used for conventional Raman spectroscopy. A wide range of experiments designed to probe structure, topology and composition of medical species using SERS microscopy can readily be envisioned. Some of these currently being studied by us are as follows: (1) development of new types of SERS-active substrates, particularly applicable to biomedical samples, and their analytical and diagnostic applications;[21–23,43–45] (2) modelling of intracellular interactions, which includes SERS analysis of the structure of antitumour drug–target complexes in terms of the biological effects of the drugs;[22,46–50] (3) studies of living cells and drug pharmacokinetics, which includes the determination of the distribution of drugs within the living cell;[22,46,57,50–55] a SERS microprobe has been used for such studies; and (4) study of cell membrane components,[21,22,56–60] which includes the ability to observe SERS from the membrane constituents which can interact with the surface of SERS-active substrates (sialic acid residues, terminating polysaccharide chains of membrane glycoproteins, membrane-bound targets for antitumour drugs, membrane-bound integral proteins, etc.).

SERS spectroscopy of antitumour drug–target complexes and biological effects

Many DNA intercalators have been shown to have antitumour activity.[61] Despite extensive efforts in analogue synthesis, the antitumour activity of these drugs is not fully understood. No single known parameter (e.g. DNA-binding strength, drug hydrophobicity, ability to inhibit DNA synthesis) is correlated with drug cytotoxicity or antitumour activity. However, the structural specificity of the drugs was clearly noted and the biological activity has been attributed to the formation of the intercalation complexes between the chromophore framework and base pairs of DNA.[62] The changes in the overall structures of the drug–target complexes amplify small chemical differences between antibiotics and provide a possible explanation for the differences in the clinical activity of the drugs.[63]

The SERS technique has become very attractive for investigation of the topology of fluorescent drug–DNA complexes because of the short-range character of the Raman enhancement and the possibilities of quenching of fluorescence in the SERS sample compartment. Sequaris *et al.*[64] were the first to analyse the SERS spectra of complexes of some Pt-coordinated compounds with DNA and to correlate the antitumour activity of these species with their ability to intercalate inside a DNA double helix. SERS spectra of some anthracyclines systematically used in the clinical treatment of cancer have been reported by Smulevich and co-workers,[65,66] Nonaka *et al.*[67] and Nabiev and co-workers.[22,49] The well detailed SERS spectra of adriamycin,[22,65,67] THP-adriamycin,[22] aclacinomycin[22,67] (Fig. 4) and some derivatives[65,66] allowed a nearly complete vibrational assignment of the resonance Raman-active modes to be made. Models of the intercalation between some drugs and DNA have been proposed and were found to be consistent with X-ray crystallographic data.[22,65–67]

We shall illustrate the capabilities of SERS spectroscopy with an example of a recent comparative study of two anticancer drugs, structurally related to anthracycline antibiotics, aclacinomycin and saintopin (Fig. 4).[49]

The decrease of SERS intensity on intercalation of the drug into DNA has been well documented and explained in terms of the short-range character of Raman enhancement in a colloid system.[22] This effect was first observed by Sequaris *et al.*[64] and used by us for studies of the topology of membrane proteins and drug–target complexes.[22] In this sense aclacinomycin belongs to the deeply intercalating chromophores. The SERS intensity of its complex with DNA [at a drug/DNA (base pairs) ratio of 1:40] is decreased about 20-fold compared with the SERS intensity of the free drug.[49] This was not the case for saintopin. We were able to record SERS spectra of its complex with DNA with a large excess (200-fold in moles of the base pairs) of the DNA duplex. At this ratio all the molecules of the drug are considered to be intercalated.[68] The SERS spectra of the complex show some decrease in intensity on saintopin interaction, but not more than 30% from

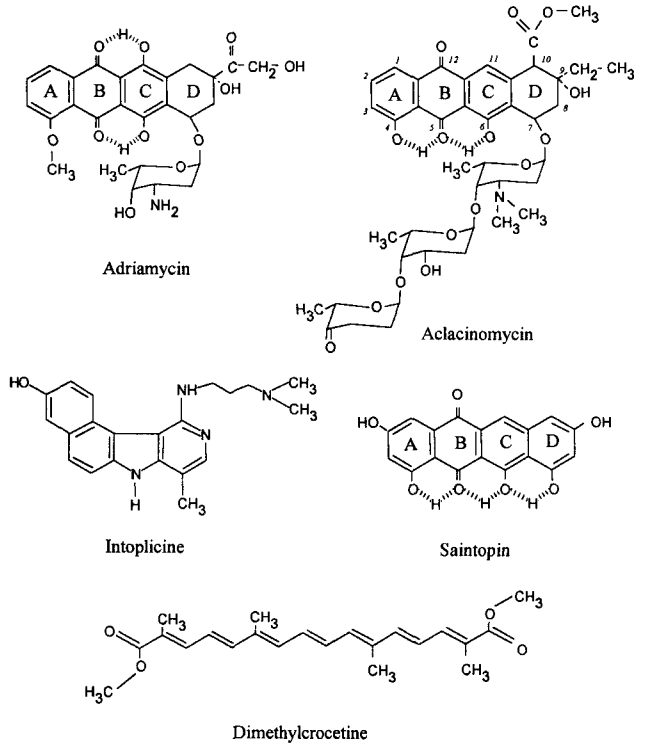

Figure 4. Structures of some antitumour drugs being discussed in the review.

the SERS intensity of the free drug. In contrast to aclacinomycin, the saintopin chromophore seems not be deeply buried in the double-stranded helix.[49]

On complexation of aclacinomycin with DNA, the following conclusions have been drawn from the SERS spectral changes:[49] (i) a new hydrogen bond between one OH group of the chromophore and functional group of DNA appears; the system of intramolecular hydrogen bonds of bonded aclacinomycin includes only one hydrogen bond (between the carbonyl group and the adjacent OH group), in contrast to the free drug, which has hydrogen bonds between the carbonyl group and two adjacent OH groups (Fig. 4); (ii) π-π interaction between the chromophore and DNA base pairs induces additional stabilization of the intercalation complex; and (iii) the free carbonyl group (Fig. 4) is buried in the interior of DNA.

We have proposed the following model (Fig. 5, left) of orientation and conformation of aclacinomycin chromophore in the interior of DNA. The free carbonyl group and chelate system of the chromophore are both buried deeply inside the double-stranded helix. In this configuration the COH group of the C-ring of aclacinomycin is hydrogen bonded with the C=O group of thymine, which is not involved in the inter-base hydrogen bonding in the T–A base pair.

As far as saintopin is concerned only a portion of the overall chromophore is involved in the intercalation (Fig. 5, right). This portion is formed by rings A and B (Fig. 4) and includes the OH $\cdots$ O intramolecular bond and the free carbonyl group. The periphery OH group of ring D (Fig. 4) is not buried inside the DNA double helix, being readily accessible to the silver surface. No evidence of redistribution of intramolecular hydrogen bonds of saintopin or the formation of new hydrogen bonds between the chromophore and DNA on intercalation could be found. The π–π interaction between the saintopin chromophore and DNA base pairs seems to provide the main contribution in the fixation of the saintopin–DNA intercalation complex (Fig. 5, right).

The following differences in the biological effects of the drugs[61,68] have been explained in terms of the differences between their intercalation modes revealed by SERS data:[49] (i) aclacinomycin shows induction of the DNA–topoisomerase II cleavable complex at a much lower concentration of the drug than for saintopin; (ii) saintopin induces a cleavable complex with both DNA–topoisomerases I and II, whereas aclacinomycin does not; and (iii) aclacinomycin inhibits the DNA–topoisomerase II cleavable complex at a high concentration of the drug whereas saintopin does not.

Cell–virus interactions. SERS analysis of sialic acid residues

It has been proposed that the interaction of organic molecules with the surfaces used for SERS experiments may be an adequate model for the study of the interfacial behaviour of biomolecules *in vivo*.[16]

The position of sialic acid (SA) residues (Fig. 6), terminal sugar of the oligosaccharide chains of the glycoproteins and glycolipids,[69] makes them accessible to the metal surface in SERS-active systems. SA residues mediate a variety of biological processes. Sialyloligosaccharides serve as receptor determinants for influenza and other viruses.[70] Oncotransformation and some somatic diseases are accompanied by distinct changes in sialylated glycoconjugates.[71]

Influenza virus infection is initiated by the specific recognition by the virus of the SA residues attached to the host cell glycoproteins or to the glycolipids.[72] Totally synthetic polyvalent inhibitors of viruses which are more potent than natural sialylglycoproteins were synthesized on the basis of water-soluble polymers containing different numbers of SA residues (Fig. 6).[73] The existence of a sharp optimum value for the density of SA residues in the polymer carrier, giving maximum inhibition of the receptor-binding activity of the influenza virus, has been demonstrated[73] (Fig. 6).

We have recorded SERS spectra from glycosides of the SA molecule (monomeric units coupled with the polymer carrier of the synthetic inhibitors).[56] The signal disappeared when the eighth and ninth hydroxyls of the

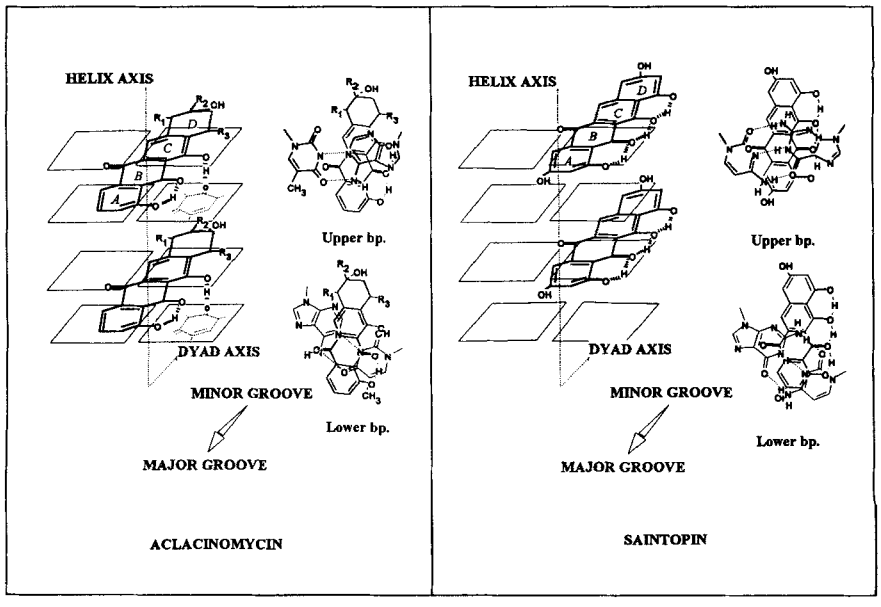

Figure 5. Proposed models of the intercalation between aclacinomycin and DNA and saintopin and DNA. For orientation of chromophores between DNA base pairs see the structures on the right. X-ray crystal data of related anthracyclines[63] have been used. $R_1 = COOCH_3$; $R_2 = CH_2CH_3$; R_3 = trisaccharide residue.

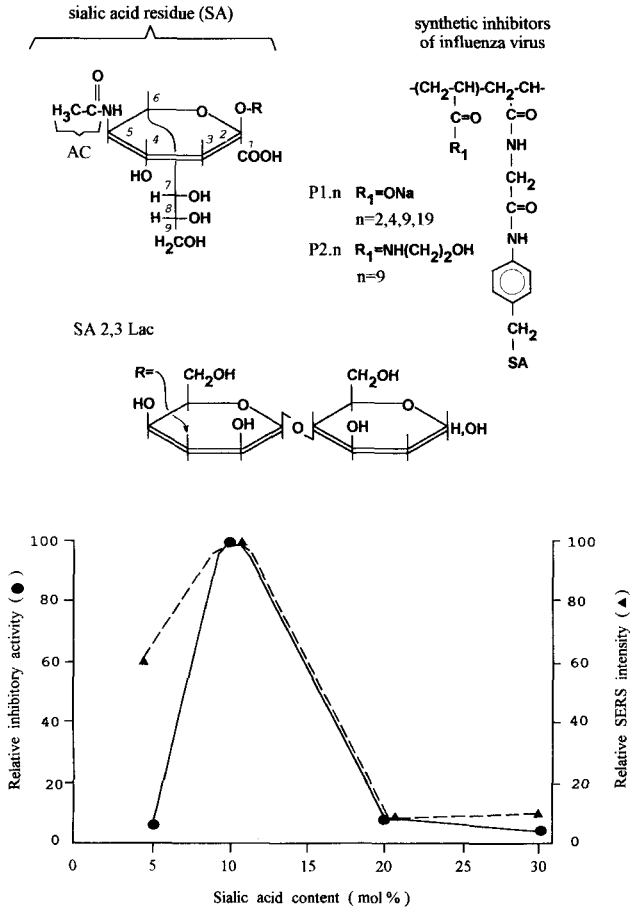

Figure 6. Correlation between inhibitory activity of synthetic polymers and their SA residue content with the intensities of their SERS spectra. Reproduced with permission from Nabiev *et al.*[22] Copyright (1993) John Wiley & Sons, Ltd.

molecule (Fig. 6) were blocked by methyl groups. The same molecular compartment is hydrogen-bonded in the viral receptor binding site and plays a role in the formation of a specific complex between SA and viral haemagglutinin (HA) glycoprotein.[72] It has been found that the patterns of interaction of SA molecules with the surface of the silver hydrosol and with the binding site of haemagglutinin receptor are similar.

We have found good correlations between the SERS intensity in the spectra of the polymers with different contents of SA residues and their biological activities (Fig. 6). A very large increase (*ca* 50-fold) of the biological activity of the polymers with increase in SA content from 5 to 10 mol% (Fig. 6) is due to the cooperative nature of the interaction between the virus and SA. Viral HA can interact with more than one SA residue when the distance between two neighbouring SA molecules decreases. In this case the relatively small increase (*ca.* twofold) of the SERS intensity is determined by the increase in the SA density on the carrier.

The sharp decrease (*ca.* tenfold) of the biological activity of the polymers with 20 and 30 mol% contents of the SA residues (Fig. 6) and a similar decrease in the SERS intensity for these polymers corresponds to a decrease in the amount of the SA glycerol moieties which are situated on the surface of the polymers and, therefore, can interact with receptor binding sites of viral HA. However, it should be noted that the intensity of the SERS signals for a polymer with an uncharged carrier containing 10 mol% of SA is extremely low (Fig. 6). This means that the polymer with uncharged carrier and a relatively small content of SA molecules has a conformation with SA residues buried in the polymer interior. Hence the behaviour of the charged SA-containing polymers can be explained by their conformational transitions from a linear form stabilized by the negative charges of the polymer carrier to the non-linear form with buried SA residues. This conformation appears when the SA content exceeds some critical value.

We have also found a good correlation between SERS intensities and biological activities for polymers with different charged carriers and optimum SA content. The deviations of SERS relative intensities from the values of relative biological activity are within 20% for all cases (Table 1).

SERS spectra of two human sialyl α_1-acid glycoproteins (Fig. 7) isolated from a blood serum of healthy donors (n-AGP) and from an ascitic fluid of stomach cancer patients (c-AGP) have been recorded.[56] After removal of the SA residues from the sugar chains both n-AGP and c-AGP gave identical spectra with the intensities dramatically decreased. These data indicate that in the SERS-active media the asialo part of the glycoproteins makes a negligible contribution to the SERS spectrum and the spectra are determined only by the vibrational bands of SA residues. Normal and cancer AGP differ from each other in SA content. Higher SERS absolute intensity for the cancer AGP as compared with the normal AGP correlates well with the diffferent SA content in these two glycoproteins.[56]

The results presented in this section demonstrate that SERS spectroscopy may be used for the rapid analysis of biological activity of some inhibitors of viruses. The short-range mechanism of Raman cross-section enhancement at the adsorption on the silver hydrosol used permits the analysis of the accessibility of the SA residues in sialylated macromolecules to water. SERS spectroscopy also provides information about the spatial disposition of SA residues relative to the polymer carrier. In addition, SERS spectroscopy is sensitive to the changes in the content of branching sialylated sugar chains in sialyglycoproteins. Thus, SERS spectra provide information about the spatial organization of SA residues on polymer carriers.

The micro-SERS method has been used to detect SA residues on the membrane of a living cell.[56] The population of myeloma X63 cells was incubated with the aggregated silver hydrosol. The SERS spectrum of the cell was determined by the signals of SA residues and the band positions correlate well with the SERS spectrum of membrane sialylated α_1-acid glycoprotein (Fig. 7). The SERS microprobe can be used as a rapid detection and conformational analysis technique for SA residues in a cell membrane for earlier diagnosis of some diseases, including oncodiagnostics.

Extracts of ocular lenses

Various fluorescent pigments are believed to be present in pathologically afflicted human lenses. These compounds presumably induce protein aggregation by

Table 1. Correlation between SERS intensities and inhibitory activity for polymers with different charged carriers and optimum contents of sialic acid residues

General structural formula	Radical (R)	Relative inhibitory activity	Relative SERS intensity
	HOOCCHCH$_2$- (with benzene ring)	100	100
-[-CH$_2$-CH-]$_{12}$-CH$_2$-CH			
C=O	Gal β_1 – O(CH$_2$)$_3$ [a]	14	11
NH			
R	HOOCCHCH$_2$CH$_2$COOH	70	78
CH$_2$			
C=O			
NH	NaCO$_2$O(CH$_2$)$_6$	9	11
(benzene ring)	NaSO$_3$O(CH$_2$)$_2$	23	27
CH$_2$			
SA			

[a] Gal = galactose.

acting as covalent, non-disulphide links (for a review, see Ref. 4). SERS spectroscopy has been found to be a powerful tool for the selective analysis of crude biomedical extracts such as extracts from human and animal eye lenses.[74,75]

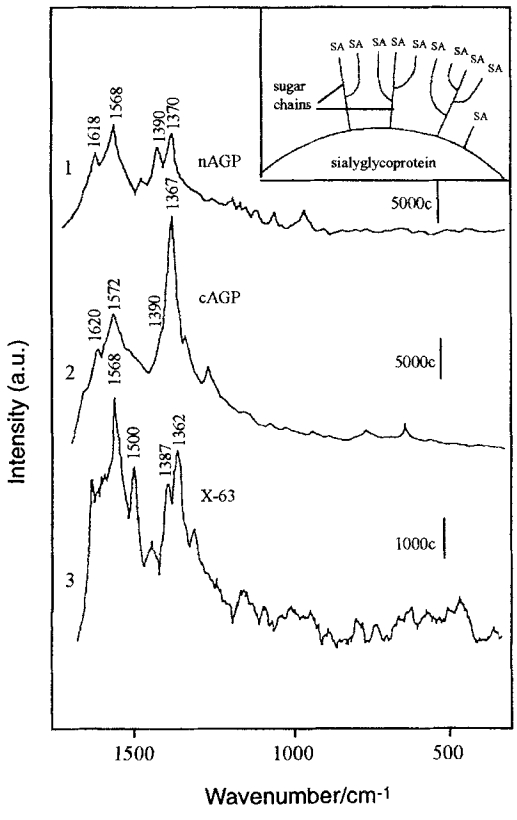

Figure 7. SERS spectra of the sialylated α_1-acid glycoproteins isolated from healthy donors (n-AGP, 1) and tumour patients (c-AGP, 2), and of a suspension of X63 cancer cells incubated with a silver hydrosol (3). Adapted with permission from Sokolov *et al.*[56] Copyright (1993) Society for Applied Spectroscopy.

SERS spectra for all the possible model pigments believed to be present in normal and cataractous human and animal ocular lenses have been recorded.[74] The SERS spectra were found to be sufficiently different to allow pigment identification on the basis of SERS data alone. Moreover, new chromophores, the structures of which are at present unknown, were found to be involved in lens pigmentation.[74]

SERS spectra of extracts from chipmunks, normal human and cataractous human eye lens and different low-molecular-weight chromatographic fractions of extracts have been studied.[75] Mass spectrometric characterization of low-molecular-weight pigments from these extracts was done to assist the detailed assignment of the bands in the SERS spectra of extracts and for the structural characterization of the pigments detected by SERS spectroscopy. We also compared SERS spectra of purified fractions with those of appropriate model compounds.[75] The mass spectrometric results were consistent with the conclusions drawn from the SERS data.

SERS microprobe approach

Van Duyne *et al.*[41] originally presented the idea of coupling the Raman microprobe with SERS. Calculated detection limits were less than 1 amol in the probe beam, which corresponds to as little as 10^5 molecules, and were *ca.* 600 molecules[42] for compounds excited in the region of their electronic transition (surface-enhanced resonance Raman effect). These detection limits show that coupling SERS and Raman microprobe spectroscopy is very promising for analysis of drugs pharmacokinetics within living cells.

We did not find any significant sample degradation effects in our SERS experiments with water-soluble and membrane proteins, nucleic acids or cells.[22] Once a stable SERS-active medium has been formed, direct photothermal or photochemical damage is minimal

even for spectra excitation in green, blue or violet regions. This can be explained by the very large Raman cross-section enhancement especially for the compounds with electronic transitions in the visible region. Hence the laser power on the level of 1 μW (irradiance *ca.* 0.5 kW cm^{-2}) has been used routinely in our SERS microprobe experiments[22,47,50] (compare with *ca* 5 MW cm^{-2} used in conventional Raman microscopy).[7–12] Thus the irradiance used for the SERS microprobe is 10^4 times less than for a conventional Raman microprobe.

SERS-active substrates used with the Raman microprobe (hydrosols, island films, nuclear pores, etc.) have metal particles and a size distribution on a submicrometre scale.[21–23] Raman microscopy probe areas are as small as *ca.* 1 μm^2 on the surface. Hence the SERS-active surface needs to be area independent for SERS intensity enhancement if any degree of reproducibility is to be expected.

The chemical mechanism of enhancement depends on atomic-scale roughness of the surface (less than 0.5 nm), that is, adatoms and clusters of adatoms.[24] These centres of adsorption are distributed regularly on the working area of a SERS-active substrate and the Raman enhancement due to the 'chemical' mechanism must be area independent. As demonstrated by Van Duyne *et al.*,[41] the same is true for the electromagnetic component of SERS enhancement. The area independence of the Raman enhancement coming from the electromagnetic field increasing near the submicrometre defects of a metal surface might at first seem unexpected, but this has been established by analysis of the SERS intensity expression for an infinitesimal area element on the surface.[41]

Living cells and drug pharmacokinetics

The SERS spectra of a number of antitumour drugs have been extensively studied and the results have been summarized.[22,27]

One of the most recent and important discoveries in the field of cancer research has been the identification of DNA topoisomerases as targets for several classes of antitumour drugs.[78,79] DNA topoisomerases (Topo I and Topo II) are nuclear enzymes that interconvert topological isomers of DNA by breaking and releasing phosphodiester bonds. They are thus involved in transcription, replication, chromosome segregation and DNA repair.[79] We were able to record the micro-SERS spectra of some antitumour drugs, inhibitors of topoisomerases, in living cancer cells and to compare them with those of its complexes with the DNA and Topo II *in vitro*.[50] Spectral differences for intoplicine complexes with the targets within the nucleus and the cytoplasm have been identified and found to be similar to those observed *in vitro* between the drug in its free form and in the ternary complex with DNA and toposiomerase. It was shown that within cells, intoplicine interacts with Topo II in the nucleus whereas it remains in a free form in the cytoplasm.

When the species are adsorbed on silver island films, only a small decrease in the signal intensity (about 35%) for the molecules with a high extinction coefficient for an electronic transition in the visible region, and at distance of *ca.* 5 nm from the silver surface, has been observed.[43] This confirms that the enhancement mechanism here is primarily long-range electromagnetic in origin and it would be reasonable to use silver island films for studies of corresponding species within the living cells.

After the deposition on the silver island film of K562 and Friend cells previously treated with dimethylcrocetine (DMCR), the signal of the pigment can be detected in the nucleus and in the cytoplasm of the cells.[22,53] The spectra demonstrated accumulation of DMCR in the cytoplasm of Friend cells but the absence of this drug in their nuclei. Moreover, new spectral components appeared in the spectra of the intracellular pigment as compared with the free DMCR. For the K562 strain the signals from DMCR located in the nucleus or in the cytoplasm were comparable in inten-

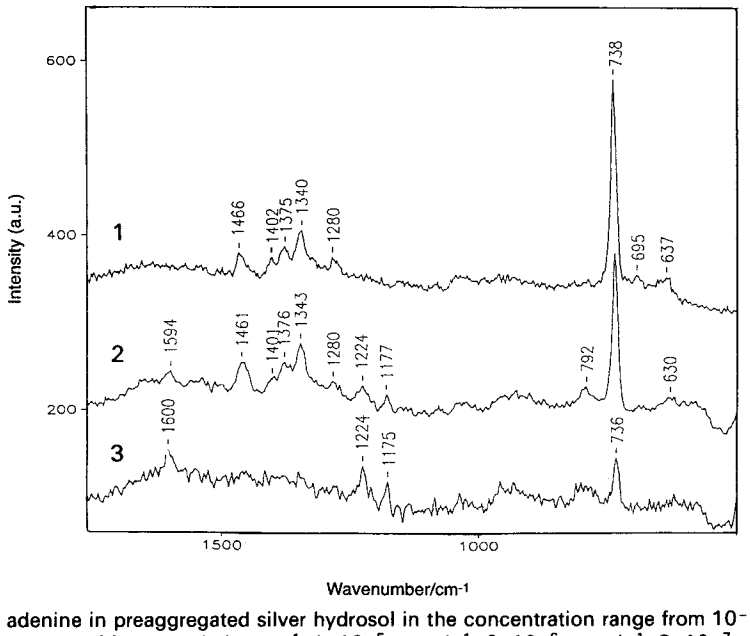

Figure 8. FT-SERS spectra of adenine in preaggregated silver hydrosol in the concentration range from 10^{-5}–10^{-7} mg ml^{-1}. Laser excitation at 1064 μm; laser power, 500 mW; 100 accumulations s^{-1}. 1: 10^{-5} mg ml^{-1}; 2: 10^{-6} mg ml^{-1}; 3: 10^{-7} mg ml^{-1}.

sity. Thus, SERS spectra revealed the difference in the modes of interaction of this drug with diverse cell strains and made an evaluation of its penetration inside the nucleus or the cytoplasm.[22]

We have used the liquid SERS-active substrate, silver hydrosol, for the SERS microprobe analysis of the interaction of doxorubicin (antitumour drug, routinely using in clinical trials) with living cancer cells.[22,47] The SERS spectrum of living cells with doxorubicin in nuclei has been found to be very different from that of cells with doxorubicin in cytoplasm but could be correlated with the spectrum of the *in vitro* complex of doxorubicin with calf thymus DNA. This means that doxorubicin in cytoplasm has a target which is different from its target (DNA) in the cell nucleus.[22]

FT-SERS spectroscopy

Applications of FT-Raman spectroscopy in a wide range of medical and pharmaceutical sciences are now well known (see the first part of this review). Nevertheless, the main disadvantage of conventional Raman spectroscopy, the low signal level, applies of course to FT-Raman spectroscopy also.[76] Moreover, the strong absorption of 1.064 μm laser radiation in water, produces some difficulties in recording NIR–FT-Raman spectra of aqueous solutions and suspensions of biomedical species. The development of the FT-SERS technique permits these problems to be circumvented.

We have used silver hydrosols, previously optimized for operating in the NIR region, for recording FT-SERS spectra. Well resolved FT-SERS spectra of nucleotides (adenine, guanine, cytosine and thymine) have been recorded at concentrations as low as 10^{-5} M.[23] A slightly higher, but 3–4 orders of magnitude less then for conventional NIR–FT-Raman spectroscopy, concentration has been used for recording of FT-SERS spectra of amino acids.[23] The detection limit of some compounds could be very low when FT-SERS is used. We were able to record a FT-SERS spectrum from aqueous solution of adenine (Fig. 8) at a concentration as low as 10^{-7} mg ml^{-1} (*ca.* 10^{-10} M). As far as we know, such a low limit of detection has never been achieved before for aqueous solutions of any compounds studied by FT-Raman spectroscopy.

CONCLUSION AND OUTLOOK

As is clear from this review, the use of Raman spectroscopy as a practical biomedical technique is already a reality. With further improvements in SERS-active substrate preparation and instrumentation, Raman spectroscopy will not only complement the other biomedical methods but also exhibit the attractive features of superior mass sensitivity, molecular specificity and *in vivo* applicability.

Acknowledgement

We gratefully acknowledge the contributions of the postdoctoral fellows and colleagues in our laboratories both at Reims University and at the Shemyakin Institute in Moscow. It is a pleasure to record our thanks to H. Morjani, J. F. Angiboust and S. Charonov (Reims University) and K. Sokolov and A. Feofanov (Shemyakin Institute). We also thank P. Tarantilis for providing us with the sample of dimethylcrocetine. We also gratefully acknowledge funding from the ARC (Association pour la Recherche Contre le Cancer, Villejuif, France), Grant No. 6225, for this programme.

REFERENCES

1. N.-T. Yu, B. H. Jo, R. C. C. Chang and J. D. Huber, *Arch. Biochem. Biophys.* **160**, 614 (1974).
2. K. A. Hartman, N. W. Clayton and G. J. Thomas, Jr, *Biochem. Biophys. Res. Commun.* **50**, 942 (1973).
3. G. J. Rosasco, in *Advances in Infrared and Raman Spectroscopy*, edited by R. J. H. Clark and R. E. Hester, Vol. 7, Chap. 4, pp. 223–282. Wiley–Heyden, London (1980).
4. S. Nie, K. L. Berbauer, J. J. Ho, J. F. R. Kuck and N. T. Yu, *Spectoscopy* **5** 24 (1990).
5. R. R. Alfano, C. H. Liu, W. L. Sha, H. R. Zhu, D. L. Atkins, J. Cleary, R. Prudente and E. Cellmer, *Laser Life Sci.* **4**, 23 (1991).
6. Y. Ozaki, A. Mizuno, H. Sato, K. Kawauchi and S. Muraishi, *Appl. Spectrosc.*, **46**, 533 (1992).
7. G. J. Puppels, A. Huizinga, H. W. Krabbe, H. A. de Boer, G. Gijsbers and F. F. M. de Mul, *Rev. Sci. Instrum.* **61**, 3709 (1990).
8. G. J. Puppels, W. Colier, J. H. F. Olminkhof, C. Otto, F. F. M. de Mul and J. Greve, *J. Raman Spectrosc.* **22**, 217 (1991).
9. G. J. Puppels, F. F. M. de Mul, C. Otto, J. Greve, M. Robert-Nicoud, D. J. Arndt-Jovin and T. M. Jovin, *Nature (London)* **347**, 301 (1990).
10. G. J. Puppels, J. H. F. Olminkhof, G. M. J. Sergers-Nolten, C. Otto, F. F. M. de Mul and J. Greve, *Exp. Cell. Res.* **195**, 361 (1991).
11. G. J. Puppels, H. S. P. Garritsen, G. M. J. Segers-Nolten, F. F. M. de Mul and J. Greve, *Biophys. J.* **60**, 1046 (1991).
12. G. J. Puppels, H. S. P. Garritsen, J. A. Kummer and J. Greve, *Cytometry* **14**, 251 (1993).
13. S. A. Asher, *Anal. Chem.* **65**, 59A (1993).
14. S. A. Asher, *Anal. Chem.* **65**, 201A (1993).
15. F. Sureau, L. Chinsky, C. Amirand, J. P. Ballini, M. Duquesne, A. Laingle, P. Y. Turpin and P. Vigny, *Appl. Spectrosc.* **44**, 1047 (1990).
16. E. Koglin and J.-M. Sequaris, *Top. Curr. Chem.* **134**, 1 (1986).
17. T. M. Cotton, in *Surface and Interfacial Aspects of Biomedical Polymers*, edited by J. Andrade, Vol. 2, pp. 161–187. Plenum Press, New York (1985).
18. T. M. Cotton, in *Spectroscopy of Surfaces*, edited by R. J. H. Clark and R. E. Hester, pp. 91–153. Wiley, New York (1988).
19. T. M. Cotton, J.-M. Kim and G. D. Chumanov, *J. Raman Spectrosc.* **22**, 729 (1991).
20. I. R. Nabiev, R. G. Efremov and G. D. Chumanov, *Sov. Phys. Usp.* **31**, 241 (1988).
21. I. R. Nabiev and R. G. Efremov, in *Surface-Enhanced Raman Spectroscopy. Principles and Applications*, edited by M. V. Vokenstein, pp. 1–189. VINITI, Moscow (1989).
22. I. R. Nabiev, K. V. Sokolov and M. Manfait, in *Biomolecular Spectroscopy*, edited by R. J. H. Clark and R. E. Hester, Vol. 21, Chapt. 7, pp. 267–338. Wiley, Chichester (1993).
23. I. Nabiev and M. Manfait, *Rev. Inst. Fr. Pétr.* **48**, 261 (1993).
24. A. Otto, I. Mrozek, H. Grabhorn and W. Akermann, *J. Phys., Condens. Matter* **4**, 1143 (1992).
25. R. F. Paisley and M. D. Morris, *Prog. Anal. Spectrosc.* **11**, 111 (1988).
26. T. Vo-Dinh, A. Alak and R. L. Moody, *Spectrochim. Acta, Part B* **43**, 605 (1988).
27. W. S. Sutherland and J. D. Winefordner, *J. Raman Spectrosc.* **22**, 541 (1991).
28. N.-T. Yu, D. L. De Nagel and J. F. R. Kuck, in *Biological Applications of Raman Spectroscopy*, edited by T. G. Spiro, Vol. 1, pp. 47–63. Wiley, New York (1987).

29. Y. Ozaki, *Appl. Spectrosc. Rev.* **24**, 259 (1988).
30. *Cancer Facts and Figures 1986*. American Cancer Society, New York (1986).
31. C.-H. Liu, B. B. Das, W. L. Sha Glassman, G. C. Tang, K. M. Yoo, H. R. Zhu, D. L. Atkins, S. S. Lubicz, J. Cleary, R. Prudente, E. Celmer, A. Caron and R. R. Alfano, *J. Photochem. Photobiol. B: Biol.* **16**, 187 (1992).
32. R. P. Rava, J. J. Baraga and M. S. Feld, *Spectrochim. Acta, Part A* **47A**, 509 (1991).
33. J. J. Baraga, M. S. Feld and R. P. Rava, *Proc. Natl. Acad. Sci. USA* **89**, 3473 (1992).
34. J. J. Baraga, M. S. Feld and R. P. Rava, *Appl. Spectrosc.* **46**, 187 (1992).
35. R. Manoharan, J. J. Baraga, M. S. Feld and R. P. Rava, *J. Photochem. Photobiol. B: Biol.* **16**, 211 (1992).
36. N.-T. Yu, D. C. De Nagel, P. L. Pruett and J. F. R. Kuck, Jr, *Proc. Natl. Acad. Sci. USA* **82**, 7965 (1985).
37. R. Mathies and N.-T. Yu, *J. Raman Spectrosc.* **7**, 349 (1978).
38. A. Huizinga, A. C. C. Bot, F. F. M. de Mul, G. F. J. M. Vrensen and J. Greve, *Exp. Eye Res.* **48**, 487 (1989).
39. A. C. C. Bot, A. Huizinga, F. F. M. de Mul, G. F. J. M. Vrensen and J. Greve, *Exp. Eye Res.* **49**, 161 (1989).
40. N.-T. Yu, M.-Z. Cai, D. J.-Y. Ho and J. F. R. Kuck, Jr, *Proc. Natl. Acad. Sci. USA* **85**, 103 (1988).
41. R. P. Van Duyne, K. L. Haller and R. I. Altkorn, *Chem. Phys. Lett.* **126**, 190 (1986).
42. G. T. Taylor, S. K. Sharma and K. Mohahan, *Appl. Spectrosc.* **44**, 635 (1990).
43. K. Sokolov, P. Hodorchenko, A. Petukhov, I. Nabiev, G. Chumanov and T. M. Cotton, *Appl. Spectrosc.* **47**, 515 (1993).
44. V. A. Oleynikov, K. V. Sokolov, P. V. Hodorchenko and I. R. Nabiev, in *Laser Applications in Life Sciences. Part I: Laser Diagnostics of Biological Molecules and Living Cells—Linear and Nonlinear Methods*, edited by S. A. Akhmanov and M. Poroshina, pp. 164–166. SPIE Proceedings Series, SPIE, Washington, DC (1990).
45. I. R. Nabiev and V. A. Oleynikov, *Russ. Pat.* 4683200/25-603382 (1990).
46. I. R. Nabiev, K. Sokolov, H. Morjani and M. Manfait, in *Spectroscopy of Biological Molecules*, edited by R. H. Hester and R. B. Girling, pp. 345–348. Royal Society of Chemistry, Cambridge (1991).
47. I. R. Nabiev, H. Morjani and M. Manfait, *Eur. Biophys. J.* **19**, 311 (1991).
48. I. R. Nabiev and M. Manfait, in *Raman Spectroscopy*, edited by W. Kiefer, M. Cardona, G. Schaack, F. W. Schneider and H. W. Schrotter, pp. 666–667. Wiley, New York (1992).
49. I. Nabiev, I. Chourpa and M. Manfait, *J. Phys. Chem.* (1994) in press.
50. H. Morjani, J.-F. Riou, I. Nabiev, F. Lavelle and M. Manfait, Cancer Res. (1993).—accepted.
51. M. Manfait, H. Morjani, J.-M. Millot, V.: Debal, J.-F. Angiboust and I. R. Nabiev, in *Laser Applications in Life Sciences. Part II: Lasers in Biophysics and Biomedicine*, edited by N. I. Koroteev and M. Poroshina, pp. 695–707. SPIE Proceeding Series, SPIE, Washington, DC (1990).
52. I. R. Nabiev, K. V. Sokolov, R. G. Efremov and G. D. Chumanov, in *Laser Applications in Life Sciences. Part I: Laser Diagnostics of Biological Molecules and Living Cells—Linear and Nonlinear Methods*, edited by S. A. Akhamanov and M. Poroshina, pp. 85–92. SPIE Proceedings Series, SPIE Washington, DC (1990).
53. M. Manfait, H. Morjani, R. Efremov, J.-F. Angiboust, M. Polissiou and I. Nabiev, in *Spectroscopy of Biological Molecules*, edited by R. E. Hester and R. B. Girling, pp. 303–304. Royal Society of Chemistry, Cambridge (1991).
54. J.-M. Millot, H. Morjani, J. Aubard, J. Pantigny, I. Nabiev and M. Manfait, in *Spectroscopy of Biological Molecules*, edited by R. E. Hester and R. B. Girling, pp. 305–306. Royal Society of Chemistry, Cambridge (1991).
55. M. Manfait, J.-F. Riou, H. Morjani, F. Lavelle and I. R. Nabiev, in *Raman Spectroscopy*, edited by W. Kiefer, M. Cardona, G. Schaack, F. W. Schneider and H. W. Schrotter, pp. 520–521. Wiley, New York (1992).
56. K. V. Sokolov, N. E. Byramova, L. V. Mochalova, A. B. Tuzikov, S. D. Shiyan, N. V. Bovin and I. R. Nabiev, *Appl. Spectrosc.* **47**, 535 (1993).
57. K. V. Sokolov, P. V. Hodorchenko, N. V. Bovin and I. R. Nabiev, in *Raman Spectroscopy*, edited by W. Kiefer, M. Cardona, G. Schaack, F. W. Schneider and H. W. Schrotter, pp. 682–683. Wiley, New York (1992).
58. N. G. Abdulaev, I. R. Nabiev, R. G. Efremov and G. D. Chumanov, *FEBS Lett.* **213**, 113 (1987).
59. I. R. Nabiev, R. G. Efremov and G. D. Chumanov, *Sov. Phys. Usp.*, **31**, 241 (1988).
60. I. R. Nabiev, G. D. Chumanov and R. G. Efremov, *J. Raman Spectrosc.* **21**, 49 (1990).
61. L. F. Liu, *Annu. Rev. Biochem.* **58**, 351 (1989).
62. W. J. Pigram, W. Fuller and L. D. Hamilton, *Nature (London)* **235**, 17 (1972).
63. A. H.-J. Wang, G. Ughetto, G. J. Quigley and A. Rich, *Biochemistry* **26**, 1152 (1987).
64. J.-M. Sequaris, E. Koglin and B. Malfoy, *FEBS Lett.* **173**, 95 (1984).
65. G. Smulevich and A. Feis, *J. Phys. Chem.* **90**, 6388 (1986).
66. G. Smulevich, A. Feis, A. R. Mantini and M. Marzocchi, *Indian J. Pure Appl. Phys.* **26**, 207 (1988).
67. Y. Nonaka, M. Tsuboi and K. Nakamoto, *J. Raman Spectrosc.* **21**, 133 (1990).
68. Y. Yamashita, S.-Z. Kawada, N. Fujii and H. Nakano, *Biochemistry* **30**, 5838 (1991).
69. R. Schauer, *Adv. Carbohydr. Chem. Biochem.* **40**, 131 (1982).
70. D. C. Wiley and J. J. Skehel, *Annu. Rev. Biochem.* **56**, 365 (1987).
71. R. Schauer and T. Yamakawa (Eds), *Sialic Acids*, Kieler Verlag Wissenschaft + Bindung, Berlin (1988).
72. W. Weis, J. H. Brown, S. Cussack, J. C. Paulson, J. J. Skehel and D. C. Wiley, *Nature (London)* **333**, 426 (1988).
73. M. N. Matrosovich, L. V. Mochalova, V. P. Marinina, N. E. Byramova and N. V. Bovin, *FEBS Lett.* **272**, 209 (1990).
74. S. Nie, C. G. Castillo, K. L. Berghauer, J. F. R. Kuck, I. R., Nabiev and N.-T. Yu, *Appl. Spectrosc.* **44**, 571 (1990).
75. K. V. Sokolov, S. V. Lutsenko, I. R. Nabiev, S. Nie and N.-T. Yu, *Appl. Spectrosc.* **45**, 1143 (1991).
76. P. J. Hendra, *J. Mol. Struct.* **266**, 97 (1992).
77. M. Manfait and I. Nabiev, in *Raman Microscopy*, edited by J. Corset, Chapt. 8. Academic Press, London (1994).
78. L. F. Liu, *Annu. Rev. Biochem.* **58**, 351 (1989).
79. J. C. Wang, *Biochim. Biophys. Acta* **909**, 1 (1989).